JOURNAL OF CATALYSIS **162,** 361–364 (1996)
ARTICLE NO. 0294

NOTE

Investigation of the Ensemble Effect of ZrO_2/Al_2O_3 Catalyst on Selective Synthesis of Ethylene from CO and H_2

While zirconium oxide as an acid–base catalyst has been extensively investigated for almost two decades (1–11), the use of oxide-supported zirconia in the hydrogenation of CO has not received great attention (12, 13). The alumina-supported zirconia (ZrO_2/Al_2O_3, China Patent CN1065026A) is an excellent catalyst for the selective synthesis of ethylene from CO and H_2 ($CO:H_2 = 1:4$, CO conversion: 30%). Both the selectivity to ethylene (70%) and the stability under the reaction conditions based on a 400-h testing offers intriguing prospects for commercialization of this catalyst (14, 15).

Four forms of crystalline zirconia have been reported (16–23), but only the monoclinic and tetragonal phases are often found in catalysts (17). The study on the structure of amorphous zirconia on the surface of metal oxides is still rare. Extended X-ray absorption fine structure (EXAFS) opens the possibility of structure and coordination geometry determination not possible by diffraction techniques and makes possible the observation at atomic level for such aperiodic systems with the same ease as crystals. In this paper, a combination of X-ray diffraction (XRD) and EXAFS techniques is applied to characterize zirconium oxide on the surface of ZrO_2/Al_2O_3 in an attempt to gain a comprehensive understanding of the EXAFS- and XRD-derived results and to gain a fundamental understanding of the active sites on the catalyst.

The BET surface of the γ-alumina (industrial grade, 0.7 g/ml) was 150 m^2/g. The γ-alumina-supported ZrO_2 catalyst, ZrO_2/Al_2O_3 (Zr 14 wt%) consists of fine particles (30–50 mesh) of white color with the BET surface about 210–230 m^2/g. The average pore diameter is 50 Å. Both freshly prepared catalysts with different metal loadings and the catalysts after 400 h running were investigated. Hydrogenation of CO was carried out in a stainless-steel reactor of 8 mm in diameter and 30 cm in length with an on-line GC analyzer. Four millilitres catalyst was filled. Reaction conditions were 0.8 MPa syngas ($CO:H_2 = 1:4$), 630 K, and $GHSV = 345\ h^{-1}$.

Predominantly monoclinic ZrO_2 (M-ZrO_2) and tetragonal ZrO_2 (T-ZrO_2) were prepared from $ZrCl_4$ according to the literature method (17), identified by XRD patterns. It has been found after calcination that predominantly M-ZrO_2 was generally obtained by rapid precipitation when 14 N NH_4OH was added to the solution of zirconium salt. However, in case a certain amount of NaOH was included in the NH_4OH solution, predominantly T-ZrO_2 was obtained. Preparation of the M-ZrO_2 and T-ZrO_2 was fundamentally controlled based on the finding in this key step.

Crystal M-ZrO_2 obtained commercially (analytical grade), and the samples mechanically mixed with γ-alumina and M-ZrO_2 were also used as references for XRD and EXAFS analyses. XRD experiments were performed on a Rigaku D/Max diffractometer using Cu$K\alpha$ radiation.

X-ray absorption spectra were obtained using the BL-7C facilities at the Photon Factory (Tsukuba, Japan) with a positron beam energy of 2.5 GeV and an average stored current of 250 mA. Data were recorded with a Si(111) double-crystal (sagittal focusing) monochromater in transmission mode. Spectra were recorded in four energy regions about the Zr K-edge (17998 eV): -100 to -30 eV in 15-eV steps, -30 to 70 eV in 1.0-eV steps, 70 to 700 eV in 4-eV steps, and above 700 eV in 8-eV steps. A general procedure for the EXAFS analysis has been given previously (24, 25).

XRD pattern shows two very strong peaks corresponding to $d = 3.14$ and 2.82 Å for the (111) face of M-ZrO_2 and a very strong peak corresponding to $d = 2.92$ Å for the (111) face of T-ZrO_2. Figure 1 shows the XRD patterns of ZrO_2/Al_2O_3 with different Zr loadings. A peak corresponding to $d = 2.92$ Å (T-ZrO_2) is developed when Zr loading is as high as 15 wt% and to be well resolved when Zr loading is greater than 25 wt%. For all the samples, no M-ZrO_2 is observed. However, the sample mechanically mixed with M-ZrO_2 and Al_2O_3 (Zr 10 wt%) clearly shows two very intense peaks at $d = 3.14$ and 2.82 Å for M-ZrO_2. Quantitative analysis reveals that the ZrO_2/Al_2O_3 with 25 wt% Zr loading yields only about 3 to 5% T-ZrO_2. It means that the catalyst ZrO_2/Al_2O_3 (Zr 14 wt%) in fact is dominated by an amorphous ZrO_2 phase.

M-ZrO_2 was used as a standard sample for calibrating the EXAFS-derived parameters in this work. In M-ZrO_2 (18–21), each zirconium atom is surrounded by seven nearest oxygen neighbors, four O_{II} atoms from a planar, square group, and the other three O_I form a triangle whose plane is nearly parallel to the plane of O_{II} atoms. The average Zr-O_I distance is 2.07 Å, whereas the average Zr-O_{II} is 2.21 Å. Each zirconium atom is also surrounded

0021-9517/96 $18.00

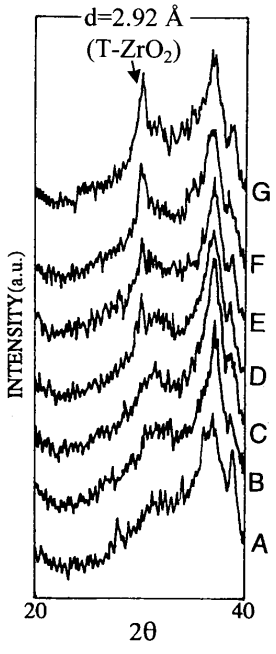

FIG. 1. X-ray diffraction pattern obtained for A, γ-Al_2O_3; and B to G, ZrO_2/Al_2O_3 with Zr loading of 3, 5, 7, 15, 20, and 25 wt%, respectively.

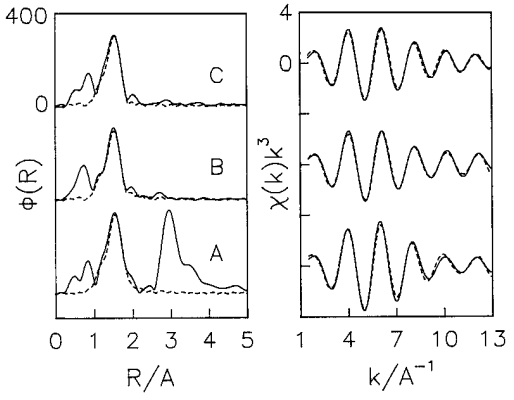

FIG. 2. Best fits (dashed lines) of the filtered first shell EXAFS spectra in *R* space (left, 1.02 to 2.37 Å) and in *k* space (right, 1.5–13.5 $Å^{-1}$ with the weight of k^3) for A, M-ZrO_2; B, the fresh ZrO_2/Al_2O_3 (Zr 14 wt%); and C, the ZrO_2/Al_2O_3 after 400 h running.

by four zirconium neighbors ranged from 3.3 to 4.0 Å. Figure 2A shows that two intense peaks are observed on the Fourier transform. The first peak centered at 1.53 Å (not corrected for phase shift) is contributed by the nearest oxygen scatterers whereas the second peak is mainly contributed by the nearest zirconium ions mixed with the next nearest oxygens. The best fits reveal 4.4 oxygens at 2.132 ± 0.009 Å and 2.6 oxygens at 2.25 ± 0.01 Å for the first peak. The average Zr–O distance of 2.18 Å and the total coordination number (CN) of 7 are thus obtained referring to the data (2.16 Å) determined by single crystal analysis (18–21).

The Fourier transform of freshly prepared ZrO_2/Al_2O_3 is shown in Fig. 2B. In comparison with that of pure M-ZrO_2, a very unique spectral feature revealed by the transform is the disappearance of the Zr–Zr coordination shell. The resulting spectrum was thought to be unbelievable when it was learned for the first time in 1991 (26) since we had tentatively proposed before the EXAFS analysis that the Zr neighbors would play an important role in the catalysis. However, the results were repeatedly confirmed by four samples at that time and by a further five samples in 1992. Undoubtedly, a conclusion derived herein is simple but very important; i.e., structurally uniform ZrO_2 ensembles containing relatively permanent –Zr–O–Zr–O–Zr– chains have no valuable effect on the catalytic properties of ZrO_2/Al_2O_3. The zirconium oxide on alumina surface, in fact, is highly dispersed although the metal loading (Zr 14 wt%) is higher than was expected for monolayer distribution (27).

The best fits to the Fourier-filtered EXAFS of freshly prepared catalyst ZrO_2/Al_2O_3 and the Fourier transform are summarized in Fig. 2B and Table 1. The best fits reveal two Zr–O shells for the catalyst; i.e., on average, each Zr site contains 4.2 oxygen neighbors at 2.105 ± 0.008 Å and 2.7 oxygens at 2.23 ± 0.001 Å. The resulting data are completely identical to those obtained for crystal M-ZrO_2 though the average Zr–O distance of 2.15 Å is shorter. Comparable experiments reveal that the pure ZrO_2 prepared by the same method as that for ZrO_2/Al_2O_3

TABLE 1

EXAFS-Derived Coordination Numbers (CN), Shell Radii (R), and Debye–Waller Factors (DW) for the Zr–O Bonds in Crystal M-ZrO_2 and the Catalysts ZrO_2/Al_2O_3

Sample (Zr wt%)	Shell	CN	R (Å)	Average R	DW ($Å^2$)	*R* factor
Crystal M-ZrO_2	Zr–O	4.4 (7)	2.132 (9)		0.004 (1)	0.14
	Zr–O	2.6 (7)	2.25 (1)	2.18	0.003 (1)	
ZrO_2/Al_2O_3	Zr–O	4.2 (5)	2.105 (8)		0.005 (1)	0.12
	Zr–O	2.7 (5)	2.23 (1)	2.15	0.004 (1)	
ZrO_2/Al_2O_3	Zr–O	4.2 (7)	2.11 (1)		0.006 (1)	0.15
After use	Zr–O	2.6 (8)	2.23 (2)	2.16	0.005 (3)	

shows very similar pictures to crystal M-ZrO_2; that is, there are two intense peaks corresponding to monoclinic form only (d = 3.14 and 2.82 Å) on its XRD pattern and a fairly intense Zr–Zr shell on its Fourier transform. The intensity of the Zr–Zr shell in the latter case is about 60% of that observed for crystal M-ZrO_2. It means that the disappearance of the Zr–Zr shell on the ZrO_2/Al_2O_3 arises from the presence of the surface lattice of the host substrate.

It is easy to see from Fig. 2C and Table 1 that the catalyst after 400 h running exhibits the same results as those of the fresh one.

XRD and EXAFS analyses consistently indicate that the surface of ZrO_2/Al_2O_3 is dominated by the amorphous ZrO_2 consisting of monoclinic-like ZrO_7 units. Since the mechanically mixed M-ZrO_2 and γ-Al_2O_3 also exhibit a good activity in the reaction (CO conversion <15%, selectivity to ethylene <60%), the much better CO conversion and ethylene selectivity reached by the catalyst are thought to originate from the significantly improved surface area of ZrO_2 and the increased bond energy of Zr–O.

Is is usually hoped for a supported oxide catalyst that, after calcination, extremely small and structurally uniform oxide ensembles will be formed on the surface. If so, just as we have previously reported for the alumina-supported iron oxide catalysts (28), a characteristic peak mainly contributed by the metal–metal coordination shell(s) must be observed on the Fourier transform following the first intense peak contributed by the metal–oxygen shell(s). The site geometry can therefore be determined by the EXAFS-derived parameters of the first peak, and the structure of the ensembles will possiblly be determined by the EXAFS-derived parameters of the M–M shell(s). However, in case the supported oxide is highly disordered, it is not surprising that only the uniform nearest coordination shell is observable. In this case, the other metal cations surrounding the central cationic sites may be randomly but almost equally distributed in a wide range; thus no particular contribution called "shell" by EXAFS can be distinguished. It seems just the case observed for the ZrO_2/Al_2O_3. Such an extremely high dispersion must be accompanied by an increased surface area. The observed value is 210–230 m^2/g, much higher than that of the zirconia and alumina (27 and 150 m^2/g, respectively). A similar phenomenon (29) is also observed for ZrO_2–TiO_2 system (BET surface > 300 m^2/g) although the properties (acidity, reducibility, and interaction with ZrO_2) of TIO_2 are known to be completely different from Al_2O_3. Other examples closely related to the topic discussed here are supported Na_2WO_4 catalysts. When the oxide support changes from SiO_2 to high ionic MgO, the catalysts show the same catalytic activity and selectivity for the oxidative coupling of methane (30, 31). These unexpected findings encourage us to postulate that geometric capability at the oxide–oxide interface is sometimes of particular importance to retain a specific active phase on surface. We have demonstrated that the (111) face of γ-alumina (32–34) matches the six coordination of iron oxides very well and makes the growth of extremely small iron entities possible (28). However, it is hard to find any geometric correlation between ZrO_2 and the Al_2O_3(111) face. Even considering the O–O distances only, it is easy to find that the distances in ZrO_7 unit of M-ZrO_2, which are ranged from 2.581 to 2.985 Å (2.74 Å on average), do not match well to the much more ordered surface of γ-alumina (O–O distance: 2.80 Å). It is thought to be a main reason for the catalyst why the high disorder is achieved. The Fourier transform of the catalyst after 400 h running clearly shows that the original spectral features of the fresh catalyst are completely remained; it is therefore still hard to understand why such a highly disordered system has a so excellent stability under the reaction conditions.

ACKNOWLEDGMENTS

The project was supported by the National Natural Science Foundation of China. We are grateful to the Photon Factory in Tsukuba, Japan, for use of the BL-7C and BL-10B facilities. We also thank Dr. T. Tanaka, Professor M. Nomura, Mr. J.-J. Lu, and Mr. Mure Te for experimental assistance.

REFERENCES

1. He,, M.-Y., and Ekerdt,, J. G., *J. Catal.* **87**, 238 (1984).
2. He, M.-Y., and Ekerdt, J. G., *J. Catal.* **87**, 381 (1984).
3. He, M.-Y., and Ekerdt, J. G., *J. Catal.* **90**, 17 (1984).
4. Maehashi, T., Maruya, K., Domen, K., Aika, K., and Onishi, T., *Chem. Lett.* 747 (1984).
5. Abe, H., Maruya, K., Domen, K., and Onishi, T., *Chem. Lett.* 1875 (1984).
6. Tanabe, K., *Mater. Chem. Phys.* **13**, 347 (1985).
7. Jackson, N. B., and Ekerdt, J. G., *J. Catal.* **101**, 90 (1986).
8. Kieffer, R., Cherry, G., and El Bacha, R., *C_1 Mol. Chem.* **2**, 11 (1987).
9. Tseng, S. C., Jackson, N. B., and Ekerdt, J. G., *J. Catal.* **109**, 284 (1988).
10. Maruya, K., Maehashi, T., Haraoka, T., Narui, S., Asakawa, Y., Domen, K., and Onishi, T., *Bull. Chem. Soc. Jpn.* **61**, 667 (1988).
11. Silver, R. G., Hou, C. J., and Ekerdt, J. G., *J. Catal.* **118**, 400 (1989).
12. Jackson, N. B., and Eherdt, J. G., *J. Catal.* **126**, 31 (1990).
13. Zhang, W.-Z., Su, G.-Q., Gao, R.-X., and Yin, Y.-Q., *J. Chem. Soc. Chem. Commun.* **8**, 622 (1992).
14. Su, G.-Q., Zhang, W.-Z., Gao, R.-X., and Yin, Y.-Q., *Chin. Sci. Bull.* **3**, 261 (1992).
15. Zhang, W.-Z., Su, G.-Q., Gao, R.-X., and Yin, Y.-Q., *J. Nat. Gas Chem.* **4**, 304 (1992).
16. Cotton, F. A., and Wilkinson, G., "Advances in Inorganic Chemistry." Wiley, New York, 1980.
17. Srinivasan, R., and Davis, B. H., *Catal. Lett.* **14**, 165 (1992).
18. McCullough, J. D., and Trueblood, K. N., *Acta Crystallogr.* **12**, 507 (1959).
19. Adam, J., and Rogers, M. D., *Acta Crystallogr.* **12**, 951 (1959).
20. Smith, D. K., and Mewkirk, H. W., *Acta Crystallogr.* **18**, 983 (1965).
21. Macdermott, T. E., *Coord. Chem. Rev.* **11**, 1 (1973).
22. Teufer, G., *Acta Crystallogr.* **15**, 1187 (1962).
23. Passerini, L., *Gazz. Chim. Ital.* **60**, 672 (1930).
24. Kou, Y., Wang, H.-L., Te, M., Tanaka, T., and Nomura, M., *J. Catal.* **141**, 660 (1993).

25. Kou, Y., Suo, Z.-H., and Wang, H.-L., *J. Catal.* **149**, 247 (1994).
26. Te, M., Kou, Y., Lu, J.-J., Su, G.-Q., Zhang, W.-Z., Tanaka, T., Nomura, M., and Yin, Y.-Q., "Photon Factory Activity Report," p. 205. KEK, Japan, 1990.
27. Xie, Y.-C., and Tang, Y.-Q., *Adv. Catal.* **37**, 1 (1990).
28. Kou, Y., Wang, H.-L., Niu, J.-Z., and Ji, W.-J., *J. Phys. Chem.* **100**, 2330 (1996).
29. Miciukiewicz, J., Mang, T., and Knözinger, H., *Appl. Catal.* **122**, 151 (1995).
30. Fang, X., Li, S., Lin, J., Gu, J., and Yang, D., *J. Mol. Catal.* **6**, 427 (1992).
31. Wang, D., Rosynek, M. P., and Lunsford, J. H., *J. Catal.* **155**, 390 (1995).
32. Lippens, B. C., and de Boer, J. H., *Acta Crystallogr.* **17**, 1312 (1964).
33. Iijima, S., *Jpn. J. Appl. Phys.* **23**, L347 (1984).
34. Iijima, S., *Surf. Sci.* **156**, 1003 (1995).

Yuan Kou[1]
Gui-qing Su
Wen-zhong Zhang
Yuan-qi Yin

State Key Laboratory for Oxo Synthesis and Selective Oxidation
Lanzhou Institute of Chemical Physics
Chinese Academy of Sciences
Lazhou 730000, China

Received September 13, 1995; revised March 21, 1996; accepted March 25, 1996

[1] To whom correspondence should be addressed.